

EXPLORING SINGLE-SONG AUTOENCODING SCHEMES FOR AUDIO-BASED MUSIC STRUCTURE ANALYSIS

Axel Marmoret, Jérémy E. Cohen*, Frédéric Bimbot

Univ Rennes, Inria, CNRS, IRISA, France.

ABSTRACT

The ability of deep neural networks to learn complex data relations and representations is established nowadays, but it generally relies on large sets of training data. This work explores a “piece-specific” autoencoding scheme, in which a low-dimensional autoencoder is trained to learn a latent/compressed representation specific to a given song, which can then be used to infer the song structure. Such a model does not rely on supervision nor annotations, which are well-known to be tedious to collect and often ambiguous in Music Structure Analysis. We report that the proposed unsupervised auto-encoding scheme achieves the level of performance of supervised state-of-the-art methods with 3 seconds tolerance when using a Log Mel spectrogram representation on the RWC-Pop dataset.

Index Terms— Autoencoders, Music Structure Analysis, Audio Signal Processing

1. INTRODUCTION

Music Structure Analysis (MSA) consists in segmenting a music piece in several distinct parts, which represent a mid-level description. Segmentation is usually based on criteria such as homogeneity, novelty, repetition and regularity [1]. In practice, MSA often relies on similarity between passages of a song summarized in an autosimilarity matrix [2–5], in which each coefficient represents an estimation of the similarity between two musical fragments.

Recently, Deep Neural Networks (DNN) have led to some high level of excitement in Music Information Retrieval (MIR) research, and notably in MSA [6, 7]. In general, DNN approaches rely on large databases which make it possible to learn a large number of parameters, which in turn yields better performance than previously established machine learning approaches. This is the consequence of the ability of DNNs to learn complex nonlinear mappings through which musical objects can be well separated [8].

However, DNNs generally learn and exploit “deep” features stemming from multiple examples used in a training

phase, and then evaluate the potential of learned features in a test phase, where no optimization is performed.

In this work, we consider a different DNN approach: we train a song-dependent autoencoder (AE), *i.e.* an AE which is specifically trained to compress a given song. By doing so, we make the hypothesis that the ability of AE to learn compressed representations of musical objects occurring within a given song will provide a set of features that are useful to infer the structure of that song.

To study the relevance of this approach, this work presents a Convolutional Neural Network (CNN)-based technique for MSA, evaluated on the RWC-Pop and SALAMI datasets [9, 10] in their audio form. Songs are represented with different features.

The rest of the article is structured as follows: Section 2 presents the formal concepts framing our work, Section 3 presents the details of our approach for music processing, Section 4 presents the segmentation process, and Section 5 reports on the experimental results on both datasets.

2. AUTOENCODERS

2.1. Basics of autoencoders

Autoencoders are neural networks, which, by design, perform unsupervised dimensionality reduction. Throughout the years, AE have received increasing interest, notably due to their ability to extract salient latent representations without the need of large amount of annotations. Recently, AE also showed great results as a generation tool [11].

An autoencoder is divided in two parts: an encoder, which compresses the input $x \in \mathbb{R}^n$ into a latent representation $z \in \mathbb{R}^m$ of smaller dimension (generally, $m \ll n$), and a decoder, which reconstructs \hat{x} from z .

In this work, layers are of two types: fully-connected, or convolutional. Convolutional layers lead to impressive results in image processing due to their ability to discover local correlations (such as lines or edges), which turn to higher-order features with the depth of the network [12]. While local correlations are less obvious in spectrogram processing [13], Convolutional Neural Networks (CNN) still perform well in MIR tasks, such as MSA [6].

*This work is partly supported by ANR JCJC project LoRAiA ANR-20-CE23-0010.

2.2. AE architecture

The tested AE is a CNN. We use the nowadays quite standard ReLU function as the activation function, except in the latent layer because it could lead to null latent variables. The encoder is composed of five hidden layers: 2 convolutional/max-pooling blocks, followed by a fully-connected layer, controlling the size of the latent space. Convolutional kernels are of size 3x3, and the pooling is of size 2x2. Convolutional layers define respectively 4 and 16 feature maps.

The decoder is composed of 3 hidden layers: a fully-connected layer (inverse of the previous one) and 2 “transposed convolutional” layers of size 3x3 and stride 2x2. A transposed convolution is similar to the convolution operation taken in the backward pass: an operation which takes one scalar as input and returns several scalars as output [14, Ch. 4]. Hence, it is well suited to inverse the convolution process. This network is represented in Figure 1.

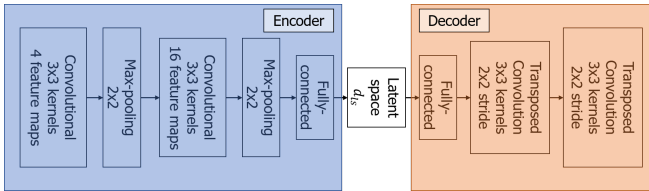


Fig. 1: Architecture of the autoencoder

3. AE FOR MUSIC PROCESSING

3.1. Motivations

The underlying idea of this work is that music structure can be related to compression of information. Indeed, a common view of music structure is to consider structural segments as internally coherent passages, and automatic retrieval techniques generally focus on finding them by maximizing homogeneity and repetition and/or by setting boundaries between dissimilar segments, as points of high novelty. In the context of compressed representations, such as AEs, each passage is transformed in a vector of small dimension, compelling this representation to summarize the original content. From this angle, similar passages are expected to be represented by similar representations, as they share underlying properties (such as coherence and redundancy), while dissimilar passages are bound to create strong discrepancies at their boundaries. Thus, we expect that compressed representations will enhance the original structure while reducing incidental signal-wise properties which do not participate to the structure.

3.2. Barwise music processing

Following our former work in [5], we process music as barwise spectrograms, with a fixed number of frames per bar.

Conversely to fixed-size frame analysis, barwise computation guarantees that the information contained in each frame does not depend on the tempo, but on the metrical positions, which is a more abstract musical notion to describe time. As a consequence, comparisons of bars are more reliable than comparisons of frames of arbitrarily fixed size as it allows to cope with small variations of tempo.

In addition, pop music (*i.e.* our case study) is generally quite regular at the bar level: repetitions occur rather clearly at the bar scale (or its multiples) and motivic patterns tend to develop within a limited number of bars, suggesting that frontiers mainly occur between bars.

Accordingly, this method relies on a consistent bar division of music. It also requires a powerful tool to detect bars, as otherwise errors could propagate and affect the performance. Results reported in [5] tend to show that the madmom toolbox [15] is efficient in that respect on the RWC-Pop dataset. Nonetheless, this processing may hinder the retrieval of boundaries based on a change of tempo.

Following this approach, each bar is represented with 96-equally spaced frames, selected from a high-resolution spectrogram (computed with a hop-length of 32 samples) [5].

3.3. Features

Music is represented with different features throughout our experiments, focusing on different aspects of music such as harmony or timbre.

Chromagram A chromagram represents the time-frequency aspect of music as sequences of 12-row vectors, corresponding to the 12 semi-tones of the classical western music chromatic scale (C, C#, ..., B), which is largely used in Pop music. Each row represents the weight of a semi-tone (and its octave counterparts) at a particular instant.

Mel spectrogram A Mel spectrogram corresponds to the STFT representation of a song, whose frequency bins are recast in the Mel scale. Mel spectrograms are dimensioned following the work of [6] (80 filters, from 80Hz to 16kHz). STFT are computed as power spectrograms.

Log Mel spectrogram A Log Mel spectrogram corresponds to the logarithmic values of the precedent spectrogram. This representation accounts for the exponential decay of frequency power.

MFCC spectrogram Mel-Frequency Cepstral Coefficients (MFCCs) are timbre-related coefficients, obtained by a discrete cosine transform of the Log Mel spectrogram. This spectrogram contains 32 coefficients, following [16].

4. STRUCTURAL SEGMENTATION

The ability of a single-song AE to separate and group bars is evaluated on the MSA task, as presented in [17].

Thereby, for a given song in a given representation, we compute latent representations z_b for all bars $1 \leq b \leq B$ of

the song. These latent representations are at the heart of the segmentation strategy, via their autosimilarity matrix.

Denoting $Z \in \mathbb{R}^{d_{ls} \times B}$ the matrix resulting from the concatenation of all d_{ls} -dimensional z_b vectors, its autosimilarity is defined as $Z^T Z$, *i.e.* the $B \times B$ matrix of the dot products between every z_b . Examples of autosimilarities are shown in Figure 2.

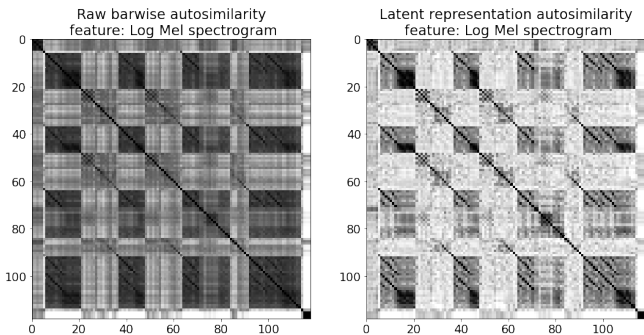


Fig. 2: Barwise autosimilarity of the raw Log Mel spectrogram (left) and of the latent representations (right), computed on the song “Pop01” from RWC-Pop.

Following the dynamic programming algorithm inspired from [18] and presented in [5], the segmentation is computed as the global maximum of the sum of all individual segments costs. The cost of each segment is obtained by applying a sliding convolving kernel on the diagonal of the autosimilarity matrix. This convolving kernel is a square matrix, the size of which is that of the potential segment.

Contrary to the novelty kernel of Foote [2], largely described in the literature [1], the proposed kernel aims at framing square blocks of high similarity, occurring when consecutive bars are similar. In that sense, while Foote’s kernel focuses on novelty, ours favors homogeneity. Still, the dynamic programming algorithm allows to find a trade-off between maximizing homogeneity of individual blocks and novelty across them as a whole. When the diagonal of the autosimilarity is structured in several self-similar blocks, the algorithm frames and partitions these blocks.

The diagonal is equal to zero, so as to disregard perfect self-similarity of each bar with itself (normalized to 1). The other elements of this kernel are designed so as to emphasize the short-term similarity in the 4 contiguous bars, and still catch longer-term similarity for long segments. This kernel performs best in comparative experiments¹ of [5].

This raw convolutional cost is combined with a(n irregularity) cost, favoring frequent segments’ sizes [18], adapted as in [5].

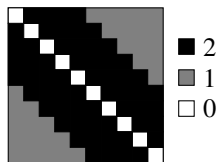


Fig. 3: Kernel of size 10

5. EXPERIMENTS

This segmentation pipeline is studied on the RWC-Pop dataset, which consists in 100 Pop songs of high recording quality [9], along with the MIREX10 annotations [19]. The best autoencoding method is also evaluated on the SALAMI dataset [10]. We focus on boundary retrieval and ignore segment labelling.

Boundaries are evaluated using the hit-rate metric, which considers a boundary valid if it is approximately equal to an annotation, within a fixed tolerance window. Consistently with MIREX standards [20], tolerances are equal to 0.5s and 3s. The hit-rate is then expressed in terms of Precision, Recall, and F-measure.

5.1. Related work

Related work mainly splits in two categories: blind and learning-based techniques.

Blind segmentation techniques, such as this work, do not use training datasets and generally focus on autosimilarity matrices. The seminal paper in this area is that by Foote [2], based on a novelty kernel, which detects boundaries as points of strong dissimilarity between the near past and future of a given instant. The strong point of this algorithm is its good performance given its relative simplicity.

Later on, McFee and Ellis made use of spectral clustering as a segmentation method by interpreting the autosimilarity as a graph and clustering principally connected vertices as segments [3]. This work performed best among blind segmentation techniques in the last structural segmentation MIREX campaign in 2016 [20]. Recently, we used tensor decomposition (Nonnegative Tucker Decomposition, NTD) as a way to describe music as barwise patterns, which then served as features for the computation of an autosimilarity matrix [5].

Still, to the best of the authors’ knowledge, the current state-of-the-art approach for the task of RWC-Pop dataset structural segmentation is a supervised CNN developed by Grill and Schlüter [6]. This technique also uses signal self-similarity as input, but in the form of lag matrices, and in conjunction with Log Mel spectrograms. Notably, this technique is trained on the SALAMI dataset only.

We compared the song-dependent autoencoders described in the present work with the aforementioned techniques. Results for [2] and [3] were computed with the MSAF toolbox [21], and boundaries were aligned to the closest downbeat (as in [5]). Results for [6] were taken from the 2015 MIREX campaign [20].

5.2. Practical considerations

Networks are developed with Pytorch 1.8.0 [22]. They are optimized with the Adam optimizer [23], with a learning rate of 0.001, divided by 10 when the loss function reaches a plateau

¹<https://gitlab.inria.fr/amarmore/musicntd/blob/v0.2.0/Notebooks/5%20-%20Different%20kernels.ipynb>

Table 1: Results of best-performing AEs and state-of-the-art on the RWC-Pop dataset. (*Results: 2015 MIREX contest [20].)

		$P_{0.5}$	$R_{0.5}$	$F_{0.5}$	P_3	R_3	F_3
Latent representations autosimilarity	Chromagram	51.8%	54%	52.3%	70.5%	73.3%	71.2%
	Mel Spectrogram	52.1%	55.3%	53.3%	73.1%	77.6%	74.7%
	Log Mel Spectrogram	59.5%	61.3%	59.9%	79.1%	81.7%	79.9%
	MFCC	54.3%	54.4%	54%	76.6%	76.4%	76%
Barwise feature representation autosimilarity	Chromagram	39.6%	38.4%	38.6%	63.8%	61.2%	62%
	Mel Spectrogram	46.4%	47%	46.3%	70.9%	71.3%	70.6%
	Log Mel Spectrogram	46.5%	46.1%	46%	72.2%	71%	71.1%
	MFCC	41.9%	40.6%	40.9%	68.1%	65.6%	66.4%
State-of-the-art	Foote [2]	42.0%	30.0%	34.5%	67.1%	47.7%	55.0%
	Spectral clustering [3]	49.2%	45%	45%	65.5%	60.6%	60.3%
	NTD [5]	58.4%	60.7%	59.0%	72.5%	75.3%	73.2%
	Supervised CNN [6]*	80.4%	62.7%	69.7%	91.9%	71.1%	79.3%

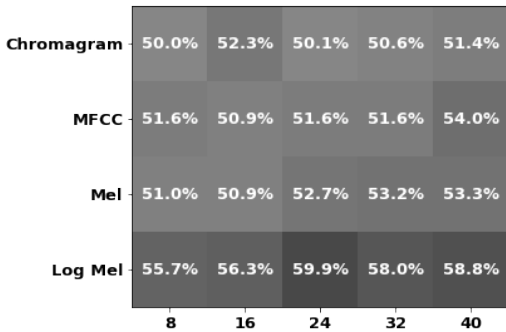


Fig. 4: F-measure with 0.5 seconds tolerance for AE with different features and latent space dimensions d_{ls} .

(20 iterations without improvement) until $1e-5$. The optimization stops if no progress is made during 100 consecutive epochs, or after a total of 1000 epochs. Each song is processed in 8-size mini-batches. All networks are initialized with the uniform distribution defined in [24], also known as “kaiming” initialization. Bars were estimated with madmom [15], and spectrograms computed with librosa [25]. All segmentation scores were computed with mir_eval [26].

The entire code for this work is open-source, and contains experimental notebooks for reproducibility². Performing 1000 epochs for a song takes between 1.5 minute (for chromagrams) and 5 minutes (for Mel/Log Mel spectrograms).

5.3. Results

Figure 4 presents results on the RWC-Pop dataset, when varying the dimension of the latent space d_{ls} . The Log Mel spectrogram clearly outperforms the other features in this task, and achieves the state-of-the-art level of performance with 3-seconds tolerance, as presented in Table 1.

Table 2 presents the results of autoencoding this Log Mel representation on the SALAMI dataset [10]. More precisely,

Table 2: Results on the SALAMI dataset (test subset of MIREX 2015), for the Log Mel spectrogram. Note: this subset contains song on which the CNN has been trained [6].

	$F_{0.5}$	F_3
Latent representation autosimilarity	36.6%	59.3%
Barwise feature autosimilarity	32%	53.9%
CNN [6] (taken from MIREX [20])	54.1%	62.3%

we used the test subset of the 2015 MIREX competition, using the upper-level annotations, and keeping for each song the annotation resulting in the best F_3 among the two available. The latent space dimension was trained on the rest of the dataset, resulting in $d_{ls} = 32$. Even though they do not reach the state of the art level, results on SALAMI still appear competitive with a tolerance of 3 seconds.

Results on both datasets are still improvable with 0.5s tolerance window. A wrong estimation at 0.5s can be due to an incorrect frontier estimation, but also to an incorrect bar estimation. This could be particularly the case for the SALAMI dataset, where music is available in very different genres and recording conditions, such as live recordings.

6. CONCLUSION

Unsupervised AEs appear as competitive schemes for Music Structure Analysis. In our experiments, the Log Mel feature outperforms the other ones, and reaches the state-of-the-art at 3 seconds tolerance on the RWC-Pop music dataset.

Future work will focus on improving the proposed paradigm using strategies such as transfer learning from a song-independent AE or exploring various network architectures. Finally, while the convolutional dynamic programming algorithm is competitive, it is unstable to small variations in autosimilarities and should be made more robust.

Altogether, we believe that these first results pave the way to an interesting paradigm using single-song AEs for the description of structural elements in music.

²<https://gitlab.inria.fr/amarmore/musicae/-/tree/v0.1.0>

7. REFERENCES

- [1] O. Nieto and al., “Audio-based music structure analysis: Current trends, open challenges, and applications,” *Trans. Int. Soc. for Music Information Retrieval*, vol. 3, no. 1, 2020.
- [2] J. Foote, “Automatic audio segmentation using a measure of audio novelty,” in *2000 IEEE Int. Conf. Multimedia and Expo. ICME2000. Proc. Latest Advances in the Fast Changing World of Multimedia*. IEEE, 2000, vol. 1, pp. 452–455.
- [3] B. McFee and D. Ellis, “Analyzing song structure with spectral clustering,” in *Int. Soc. Music Information Retrieval (ISMIR)*, 2014, pp. 405–410.
- [4] O. Nieto and T. Jehan, “Convex non-negative matrix factorization for automatic music structure identification,” in *2013 IEEE Int. Conf. Acoustics, Speech and Signal Processing (ICASSP)*. IEEE, 2013, pp. 236–240.
- [5] A. Marmoret, J.E. Cohen, N. Bertin, and F. Bimbot, “Uncovering audio patterns in music with nonnegative tucker decomposition for structural segmentation,” in *ISMIR*, 2020, pp. 788–794.
- [6] T. Grill and J. Schlüter, “Music boundary detection using neural networks on combined features and two-level annotations,” in *ISMIR*, 2015, pp. 531–537.
- [7] M.C. McCallum, “Unsupervised learning of deep features for music segmentation,” in *ICASSP*. IEEE, 2019, pp. 346–350.
- [8] E.J. Humphrey, J.P. Bello, and Y. LeCun, “Feature learning and deep architectures: New directions for music informatics,” *J. Intelligent Information Systems*, vol. 41, no. 3, pp. 461–481, 2013.
- [9] M. Goto, H. Hashiguchi, T. Nishimura, and R. Oka, “RWC Music Database: Popular, Classical and Jazz Music Databases,” in *ISMIR*, 2002, vol. 2, pp. 287–288.
- [10] J.B.L. Smith, J.A. Burgoyne, I. Fujinaga, D. De Roure, and J.S. Downie, “Design and creation of a large-scale database of structural annotations,” in *ISMIR*. Miami, FL, 2011, vol. 11, pp. 555–560.
- [11] J. Engel and al., “Neural audio synthesis of musical notes with wavenet autoencoders,” in *Int. Conf. Machine Learning*. PMLR, 2017, pp. 1068–1077.
- [12] Y. LeCun, L. Bottou, Y. Bengio, and P. Haffner, “Gradient-based learning applied to document recognition,” *Proc. of the IEEE*, vol. 86, no. 11, pp. 2278–2324, 1998.
- [13] G. Peeters and G. Richard, “Deep Learning for Audio and Music,” in *Multi-faceted Deep Learning: Models and Data*. Springer, 2021.
- [14] V. Dumoulin and F. Visin, “A guide to convolution arithmetic for deep learning,” *arXiv preprint arXiv:1603.07285*, 2016.
- [15] S. Böck, F. Korzeniowski, J. Schlüter, F. Krebs, and G. Widmer, “madmom: a new Python Audio and Music Signal Processing Library,” in *Proc. 24th ACM Int. Conf. Multimedia*, Amsterdam, The Netherlands, 10 2016, pp. 1174–1178.
- [16] B. McFee and D. Ellis, “Learning to segment songs with ordinal linear discriminant analysis,” in *ICASSP*. IEEE, 2014, pp. 5197–5201.
- [17] J. Paulus, M. Müller, and A. Klapuri, “Audio-based music structure analysis,” in *ISMIR*. Utrecht, 2010, pp. 625–636.
- [18] G. Sargent, F. Bimbot, and E. Vincent, “Estimating the structural segmentation of popular music pieces under regularity constraints,” *IEEE/ACM Trans. Audio, Speech, and Language Processing*, vol. 25, no. 2, pp. 344–358, 2016.
- [19] F. Bimbot, G. Sargent, E. Deruty, C. Guichaoua, and E. Vincent, “Semiotic description of music structure: An introduction to the quaero/metiss structural annotations,” in *53rd Int. Conf. Audio Engineering Soc.*, 2014.
- [20] “MIREX wiki,” https://www.music-ir.org/mirex/wiki/MIREX_HOME, (Accessed: Sep. 29, 2021).
- [21] O. Nieto and J.P. Bello, “Systematic exploration of computational music structure research,” in *ISMIR*, 2016, pp. 547–553.
- [22] A. Paszke and al., “Pytorch: An imperative style, high-performance deep learning library,” in *Advances in Neural Information Processing Systems 32*, pp. 8024–8035. Curran Associates, Inc., 2019.
- [23] D.P. Kingma and J. Ba, “Adam: A method for stochastic optimization,” *arXiv preprint arXiv:1412.6980*, 2014.
- [24] K. He, X. Zhang, S. Ren, and J. Sun, “Delving deep into rectifiers: Surpassing human-level performance on imagenet classification,” in *Proc. IEEE Int. Conf. Computer Vision*, 2015, pp. 1026–1034.
- [25] B. McFee and al., “librosa/librosa: 0.8.1rc2,” May 2021.
- [26] C. Raffel and al., “mir_eval: A transparent implementation of common MIR metrics,” in *ISMIR*, 2014.